The 7th International Conference on
Engineering Mechanics and Automation (ICEMA - 2023)
Hanoi, November 11, 2023

DOI: 10.15625/vap.2023.0146

A Novel Configuration of Tuned Mass Damper With Energy Harvester of Piezoelectric Stack and Force Amplification Frame

Nguyen Ngoc Linh
Faculty of Mechanical Engineering
Thuy loi university
Hanoi, Vietnam
nnlinh@tlu.edu.vn

Nguyen Dong Anh
Faculty of Engineering Mechanics and Automation
University of Engineering and Technology, VNU
Hanoi, Vietnam
ndanh0403@gmail.com

***Abstract*— The paper is concerned with a novel configuration of a tuned mass damper (TMD) equipped with an energy harvester that is a combination of piezoelectric stacks and force amplification frames connected to the TMD springs in series (TMD-PSFAF). It will be proven that this combination can be equivalent to a piezoelectric stacks in terms of dynamics. Next, the physical and mathematical models of TMD-PSFAF attached to an undamped primary structure under external excitation is established. Numerical investigation of the electromechanical system reveals that all magnification factors and voltage amplitude curves have fixed points independent of damping. Effective tuning, damping and electrical resistance ratios are then proposed.**

Keywords*— Tuned mass damper, vibration energy harvesting, piezoelectric stack, force amplification frame.

I. Introduction

Recently, vibration-based piezoelectric energy harvesters have been widely developed as a promising alternative to traditional batteries or power grids [1]-[3]. Piezoelectric multilayer stack (PS) operating in the d_{33} mode is an appropriate harvester for applications involving large loads. However, one of the major problems when using a stand-alone PS for such applications is that only a small amount of energy will be generated under direct loading due to their extremely high stiffness [4], [5]. To overcome this problem, rhomboid-shaped concave mechanisms were proposed to amplify the input force applied to the shorter axis [6], [7], [8]. However, since each linkage in these mechanisms is subject to a large compressive force due to its positive tilting angle, such type of mechanism is at high risk of local buckling [9]. To resolve the bulking problem, convex force amplification frames were proposed so that the stress applied to the frame is tensile instead of compressive [9]-[12]. The combination of PS with force amplification frame (FAF) can be considered a module which is the so-called PSFAF.

Furthermore, the integration of vibration absorbers (VA) and/or tuned mass dampers (TMD) with energy harvesters like PS has become a rising need [13]-[18]. For instance, in [16], a TMD-PS without damper attached to a damped primary structure is studied. The proposed energy harvester is a multiple-row-column PS that can be characterized by an equivalent PS. In [18], a TMD-PS attached to an undamped primary system subjected to base excitation is investigated where the PS is connected to the TMD's spring in series.

This paper is concerned with a novel configuration of TMD with PSFAF which is introduced in [19]. Modeling of the electromechanical system is implemented in Section 2. Numerical examination is carried out in Section 3. Section 4 contains a summary and conclusions.

II. Tuned Mass Damper With Energy Harvester of Piezoelectric Stack and Force Amplification Frame

A. Configuration of TMD with PSFAF

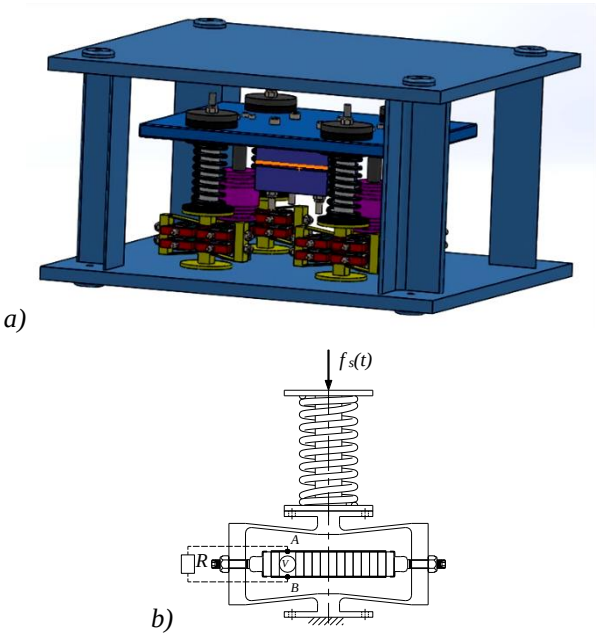

Fig. 1. TMD with PSFAF: a) mechanical configuration, b) Block of TMD's spring and PSFAF

As depicted in Fig. 1a, the proposed system in the Patent [19] deals with a TMD incorporating PSFAF. The TMD consists of a mass m_d, dampers with the damping coefficient c_d, and springs with stiffness k_d. The TMD's springs connect

to PSFAF in series (Fig. 1b). The TMD-PSFAF can be attached to a primary structure through an assembly frame using bolt joints. The working principle of the system is that the vibration of the primary structure is transferred partially vibration energy to the TMD, a part of the transferred energy is absorbed by the damper, and the other is converted to electrical energy through the piezoelectric effect. The FAF is used to amplify the output force delivered from the TMD's spring force which acts on the PS. Hence, the vibration of the primary structure is suppressed, at the same time the electrical energy amount can be enlarged.

B. Modeling of TMD's spring with PSFAF

Consider the block of TMD's spring and PSFAF which are connected in series as depicted in Fig. 1b. The physical model of the block is shown in Fig. 2a where it is subjected to an axial force f_d that delivers the force f_{d1} on TMD's spring and the force f_{d2} on the PSFAF. Assuming that each linkage of the FAF is an elastic element, has negligible mass and hinge connections at both ends (no reaction moments) while other parts can be regarded as a rigid body. Therefore, the deformations occurring in the linkages are so small that they are only axial. Denote x_s is the total deformation of the block, x_{d1}, x_{d2}, x_f, x_p are the deformations of the TMD's spring with stiffness k_{d1}, of the FAF, of the linkages with stiffness k_f, and of the piezoelectric stack with stiffness k_p, respectively. Modeling of the block with the force-voltage relationship can be developed as follows.

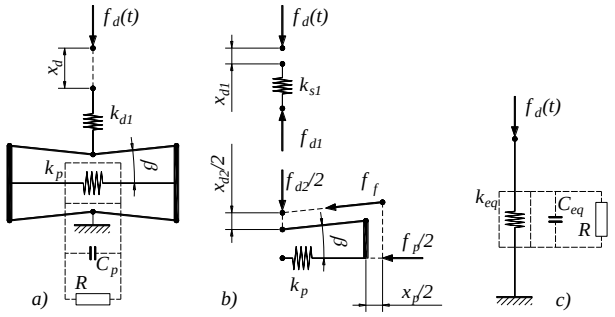

Fig. 2. Modeling of a PSFAF connected to a spring in series: a) Physical model, b) quarter free body, c) equivalent model

First, it is clear that

$$f_d = f_{d1} = f_{d2} \tag{1}$$

$$x_d = x_{d1} + x_{d2} \tag{2}$$

where:

$$f_{d1} = k_{d1} x_{d1} \tag{3}$$

Based on the geometric relationship (see Fig. 2b), the elastic force f_f of each linkage delivered from f_{d2} becomes

$$f_f = f_{d2} / (2\sin\beta) \tag{4}$$

where: β is the angle of each of the four linkages with respect to the horizontal direction, i.e., structural angle. On the other hand, the force f_p applied to the piezoelectric stack is

$$f_p = 2 f_f \cos\beta \tag{5}$$

From (4), (5), one gets the relationship between f_{d2} and f_p

$$f_p = k_A f_{d2}, \qquad k_A = \cot\beta \tag{6}$$

k_A is called the force amplification factor. Based on the energy transmission principle for FAF, the input work equals the output one, i.e. $f_{d2} x_{d2} = f_p x_p$, using (6) one has

$$\frac{x_{d2}}{x_p} = \frac{f_p}{f_{d2}} = k_A = \cot\beta \tag{7}$$

Noting (2), (3), one can extract from (7)

$$x_p = \frac{x_{d2}}{k_A} = \frac{1}{k_A}(x_d - x_{d1}) = \frac{1}{k_A}\left(x_d - \frac{f_d}{k_{d1}}\right) \tag{8}$$

The force-voltage relationship of the PS is governed by the following constitutive equations [20]

$$f_p = k_p x_p + \theta_p V \tag{9}$$

$$q = \theta_p x_p - C_p V \tag{10}$$

where: θ_p is the effective electromechanical coupling coefficient, q is the produced electric charge, C_p is the internal capacitance, and V is the voltage of the PS caused by the force f_p. From (1), (6) and (9) one has

$$x_p = \frac{f_p}{k_p} - \frac{\theta_p}{k_p} V = \frac{k_A f_d}{k_p} - \frac{\theta_p}{k_p} V \tag{11}$$

Equaling (8) and (11) yields

$$f_d = \frac{k_{d1} k_p}{k_{d1} k_A^2 + k_p} x_2 + \frac{k_{d1} \theta_p}{k_{d1} k_A^2 + k_p} k_A V \tag{12}$$

Next, substituting (11) and (12) into (10) one gets

$$q = \frac{k_{d1} \theta_p}{k_{d1} k_A^2 + k_p} x_2 - \left[\frac{C_p}{k_A} + \frac{\theta_p^2}{k_p k_A}\left(1 - \frac{k_{d1} k_A}{k_{d1} k_A^2 + k_p}\right)\right] k_A V \tag{13}$$

Equations (12) and (13) can be rewritten as

$$f_d = k_{eq} x_d + \theta_{eq} \tilde{V} \tag{14}$$

$$q = \theta_{eq} x_q - C_{eq} \tilde{V} \tag{15}$$

where:

$$k_{eq} = \frac{k_{d1}k_p}{k_{d1}k_A^2 + k_p}, \theta_{eq} = \frac{k_{d1}}{k_{d1}k_A^2 + k_p}\theta_p,$$
$$C_{eq} = \frac{C_p}{k_A} + \frac{\theta_p^2}{k_p k_A}\left(1 - \frac{k_{d1}k_A}{k_{d1}k_A^2 + k_p}\right), \tilde{V} = k_A V \quad (16)$$

One can conclude that the block of TMD's spring and PSFAF can be modeled as an equivalent PS where its constitutive equations (14), (15) are expressed in the total deformation x_d of the block, as shown in Fig. 2c. It is interesting to know that the block of TMD's spring and PS (without FAF) can also be considered as an equivalent PS, as proven in [21].

C. Modeling of undamped primary structure with TMD-PSFAF

The physical model of an undamped primary structure with TMD-PSFAF is illustrated in Fig. 3a. Denote $\bar{t}$ being the time, the harmonic external excitation $F(\bar{t})$ with amplitude F_0 and frequency Ω acting on m_s in the form of

$$F(\bar{t}) = F_0 \cos \omega \bar{t} \quad (17)$$

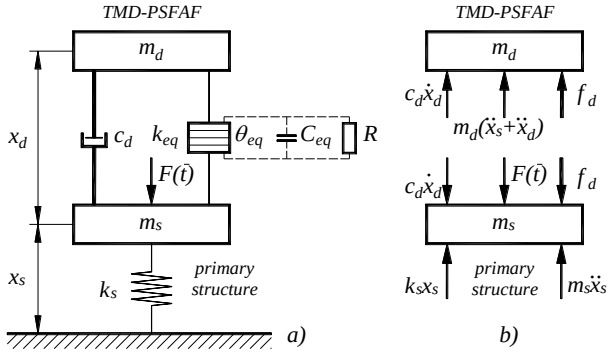

Fig. 3. Schematic of TMD-PSFAF system: a) lumped-mass model, b) equilibrium of forces

Since the block of TMD's spring and PSFAF can be modeled as an equivalent PS, the governing equations of the considered system are given by

$$m_s\ddot{x}_s - c_d\dot{x}_d + k_s x_s - k_{eq}x_d - \theta_{eq}\tilde{V} = F_0\cos(\omega\bar{t})$$
$$m_d\ddot{x}_d + c_d\dot{x}_d + k_{eq}x_d + \theta_{eq}\tilde{V} = -m_d\ddot{x}_s \quad (18)$$
$$C_{eq}\dot{\tilde{V}} + \frac{\tilde{V}}{R} = \theta_{eq}\dot{x}_d$$

Let us denote

$$t = \omega_s\bar{t}, x_s = x_1, x_d = x_2,$$
$$\omega_s = \sqrt{k_s/m_s}, \omega_d = \sqrt{k_{eq}/m_d}, \mu = m_d/m_s,$$
$$\xi_d = \frac{c_d}{2m_d\omega_d}, \beta = \frac{\omega_d}{\omega_s}, \lambda = \frac{\omega}{\omega_s}, \kappa^2 = \frac{\theta_{eq}^2}{k_d C_{eq}}, \quad (19)$$
$$v = \frac{C_{eq}\tilde{V}}{\theta_{eq}}, \alpha = \frac{1}{\omega R C_{eq}}, X_{st} = \frac{F_0}{k_s}$$

Hence the equation system (18) can be transformed into the following dimensionless system

$$\ddot{x}_1 - 2\mu\beta\xi_d\dot{x}_2 + x_1 - \mu\beta^2 x_2 - \mu\beta^2\kappa^2 v = X_{st}\cos\lambda t$$
$$\ddot{x}_2 + 2\beta\xi_d\dot{x}_2 + \beta^2 x_2 + \beta^2\kappa^2 v = -\ddot{x}_1 \quad (20)$$
$$\dot{v} + \lambda\alpha v = \dot{x}_2$$

where: the over dots now denote the derivatives regarding dimensionless time *t*. Physically, ω_s and ω_d are the natural frequency of the primary structure and the TMD-PSFAF, κ^2 is the electromechanical coupling coefficient, α is the resistance ratio, v is the transformed voltage, and $\mu, \xi_d, \beta, \lambda$ are the mass ratio, damping ratio, tuning ratio, and the ratio of excitation frequency to primary structure frequency, respectively. It is seen that the system (20) is a linear system of ordinary differential equations for three unknowns, $x_1(t), x_2(t)$ and $v(t)$. Solving (20), those responses could be obtained as follows

$$x_1(t) = A_1\cos(\lambda t + \varphi_1)$$
$$x_2(t) = A_2\cos(\lambda t + \varphi_2) \quad (21)$$
$$v(t) = A_3\cos(\lambda t + \varphi_3)$$

where: A_1, A_2, A_3 and $\varphi_1, \varphi_2, \varphi_3$ are amplitudes and phases of $x_1(t), x_2(t), v(t)$, respectively, which are given by

$$A_1 = X_{st}\sqrt{\frac{B_1^2 + B_2^2}{E_1^2 + E_2^2}}, \varphi_1 = \tan^{-1}\left(\frac{B_2E_1 - B_1E_2}{B_1E_1 + B_2E_2}\right),$$
$$A_2 = X_{st}\sqrt{\frac{C_1^2 + C_2^2}{E_1^2 + E_2^2}}, \varphi_2 = \tan^{-1}\left(\frac{C_2E_1 - C_1E_2}{C_1E_1 + C_2E_2}\right), \quad (22)$$
$$A_3 = X_{st}\sqrt{\frac{D_1^2 + D_2^2}{E_1^2 + E_2^2}}, \varphi_3 = \tan^{-1}\left(\frac{D_2E_1 - D_1E_2}{D_1E_1 + D_2E_2}\right)$$

where:

$$B_1 = \alpha(\beta^2 - \lambda^2) - 2\beta\xi_2\lambda,$$
$$B_2 = \beta^2 - \lambda^2 + 2\alpha\beta\xi_2\lambda + \kappa^2\beta^2,$$
$$C_1 = \alpha\lambda^2, C_2 = \lambda^2, D_1 = 0, D_2 = \lambda^2,$$
$$E_1 = (\lambda^2 - 1)(2\beta\xi_2\lambda - \alpha\beta^2 + \alpha\lambda^2) \quad (23)$$
$$+\mu\beta\lambda^2(2\xi_2\lambda - \alpha\beta),$$
$$E_2 = (1 - \lambda^2)(2\alpha\beta\xi_2\lambda + \kappa^2\beta^2 + \beta^2 - \lambda^2)$$
$$-\mu\beta\lambda^2(\beta + 2\alpha\xi_2\lambda + \kappa^2\beta)$$

Accordingly, the mechanical magnification factors of $x_1(t), x_2(t)$, say K_1, K_2, and the voltage amplitude factor, say v_0, are calculated by, respectively

$$K_1 = \frac{A_1}{X_{st}} = \sqrt{\frac{B_1^2 + B_2^2}{E_1^2 + E_2^2}} \quad (24)$$

$$K_2 = \frac{A_2}{X_{st}} = \sqrt{\frac{C_1^2 + C_2^2}{E_1^2 + E_2^2}} \tag{25}$$

$$v_0 = \frac{A_3}{X_{st}} = \sqrt{\frac{D_1^2 + D_2^2}{E_1^2 + E_2^2}} \tag{26}$$

It is seen from (20) that when $\kappa^2 = 0$ one gets the mechanical TMD system. Practically, the value of κ^2 is small for engineering systems. Therefore, to investigate the behavior of the undamped primary structure with TMD-PSFAF in considering $\kappa^2 \to 0$, the results of the optimal mechanical TMD [22], [23] are adopted for β and ξ_d of TMD-PSFAF

$$\begin{aligned} \beta &= \beta_{DH} = \frac{1}{1+\mu} \\ \xi_d &= \xi_{DH} = \sqrt{\frac{3\mu}{8(1+\mu)}} \end{aligned} \tag{27}$$

III. Numerical Examination

Fig. 4a and Fig. 4b depict curves K_1, K_2 given by Eqs. (24), (25), while Fig. 4c depicts curve v_0 given by Eq. (26) in the frequency domain with $\mu = 0.05, \kappa^2 = 0.01, \alpha = 1$. It is seen that all curves K_1, K_2, v_0 have fixed points independent of damping. Namely, the curve K_1 has two fixed points, say $P(\lambda_{1P}, K_{1P}) = P(0.8965, 6.524)$ and $Q(\lambda_{1Q}, K_{1Q}) = Q(1.05, 6.303)$, the curve K_2 has a fixed point $S_2(\lambda_{2S}, K_{2S}) = S_2(0.976, 21)$, while the curve v_0 also has a fixed point $S_3(\lambda_{3S}, K_{3S}) = S_3(0.976, 14.85)$.

In more detail, it is seen from Fig. 4a that K_1 has two peaks that are close to P and Q as $\xi_d = \xi_{DH}$. The height of the left peak is 6.513, while that of the right one is 6.304, corresponding to a height difference of 3.21%. As $\xi_d < \xi_{DH}$, the two peaks of K_1 are higher than K_{1P}, K_{1Q}. As $\xi_d > \xi_{DH}$, these two peaks merge into one and this single peak is still higher than K_{1P}, K_{1Q}. Thus, the tuning and damping ratios β_{DH} and ξ_{DH} keep the two peaks of the curve K_1 at approximately equal height, and they are lower than that corresponds to other considered values of β and ξ_d.

As shown in Fig. 4b, the curve K_2 also has two peaks of approximately equal height appearing in the vicinity of λ_P, λ_Q. The two peaks are higher than K_{2S} as $\xi_d < \xi_{DH}$, and merge into a single peak at the fixed point S_2 as $\xi_d > \xi_{DH}$. As $\xi_d = \xi_{DH}$, the corresponding two peaks of K_2 have nearly equal heights, say 21.71 on the left and 21.29 on the right. Since those peaks are much higher than that of K_1, it is shown that the vibration of m_s is suppressed and converted partially to the vibration of m_2.

Similarly, the curve v_0 has the same properties as that of the curve K_2 (Fig. 4c). More specially, the abscissa λ_{3S} of the fixed point S_3 is coincided with λ_{2S} of the fixed point S_2. For both curves K_2 and v_0, the two peaks tend to infinite as $\xi_d \to 0$, otherwise tend to zero as $\xi_d \to \infty$.

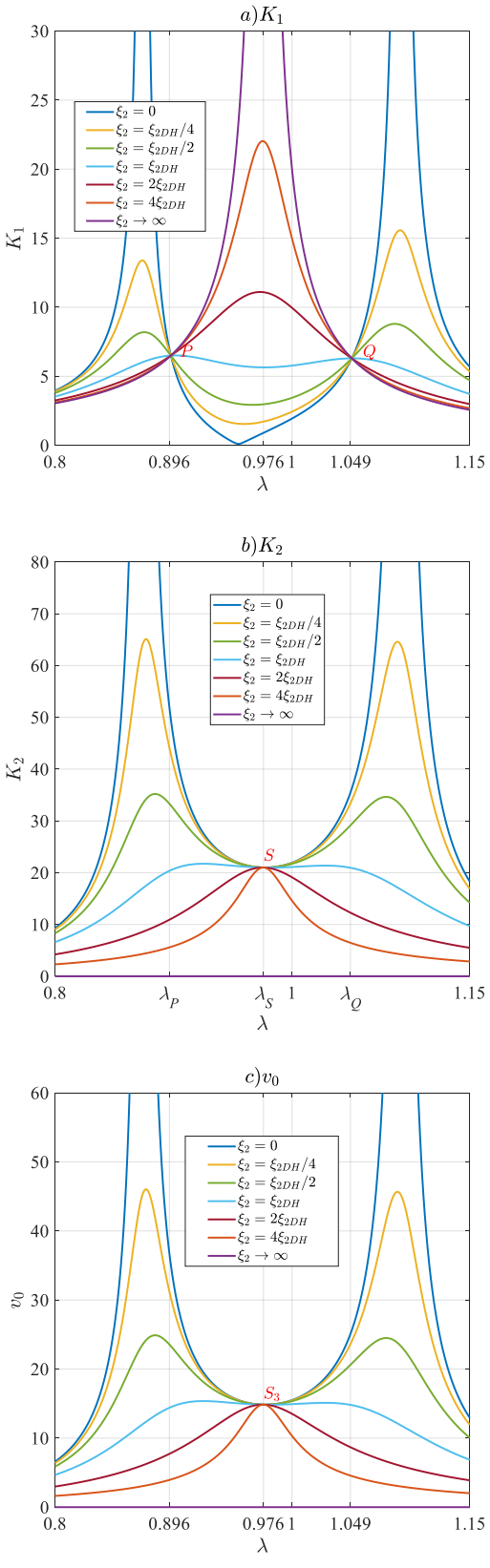

Fig. 4. K_1, K_2, v_0 versus λ with $\mu = 0.05, \kappa^2 = 0.01, \alpha = 1$ and ξ_2 varies: a) K_1; b) K_2; c) v_0

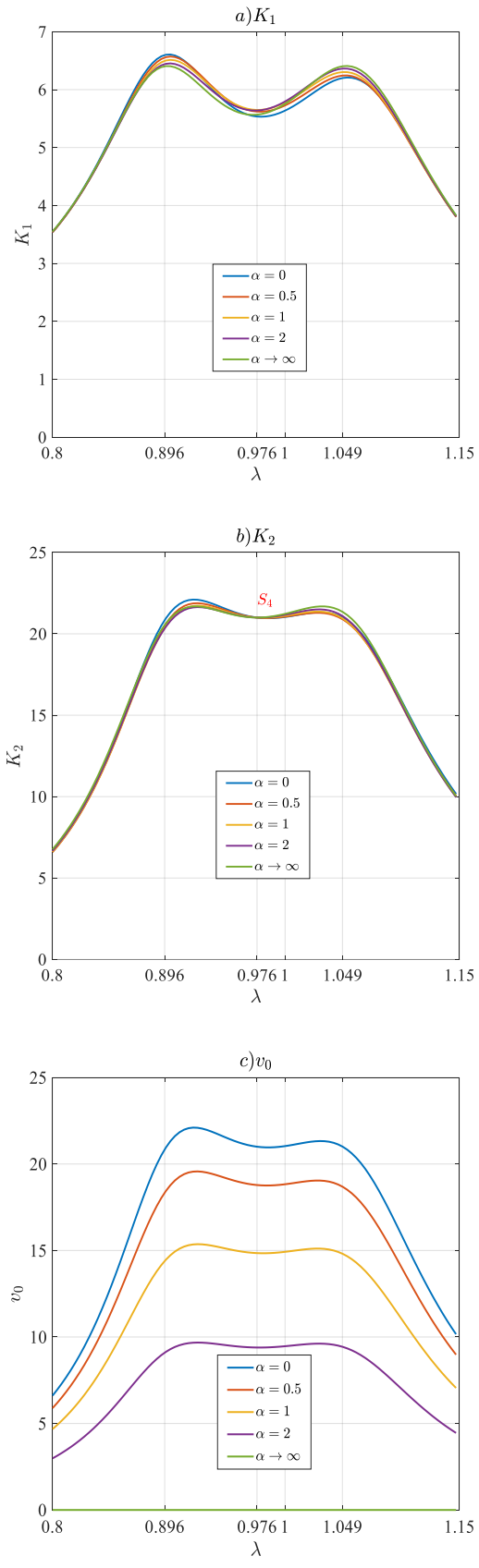

Fig. 5. K_1, K_2, v_0 versus λ with $\mu = 0.05,\ \kappa^2 = 0.01,\ \beta = \beta_{DH}, \xi_d = \xi_{DH}$ and α varies: a) K_1, b) K_2, c) v_0

Fig. 5 shows the effect of α, $\beta = \beta_{DH}, \xi_d = \xi_{DH}$, the values of μ, κ^2 are unchanged. It is known that the case $R \to \infty, \alpha \to 0$ involves an open-circuit condition, while the case $R \to 0, \alpha \to \infty$ involves a short-circuit condition. The other values of α vary from those cases. Generally, α has less effect on K_1, K_2 (Fig. 5a, b). Any change in the value of α leads to the right peak of K_1, K_2 being higher than the left one but the height difference is not large. It is interesting to see that the two peaks of K_1, K_2 have almost equal heights as $\alpha \to \infty$, i.e. 6.406 versus 6.408 for K_1, 21.68 versus 21.69 for K_2. That means $\alpha \to \infty$ may be an optimal value for vibration suppression of K_1 regarding $\beta = \beta_{DH}, \xi_d = \xi_{DH}$. However, it is emphasized that $\alpha \to 0$ corresponds to the maximum voltage, $\alpha \to \infty$ corresponds to the zero voltage (Fig. 5c), and both open- and short-circuit conditions result in zero electrical power. Besides, the larger the value of α, the smaller the voltage amplitude will be. Therefore, to ensure that the two peaks of K_1 are approximately equal in height and the voltage amplitude v_0 is large enough, the value of α should be considered in the interval [1, 2]. Moreover, K_2 has a fixed point independent of α, i.e. $S_4 = S_4(0.976, 21)$. It is found that the fixed point S_4 is coincided with the fixed point S_2.

IV. Conclusion

In the paper, the following main works and conclusions could be drawn

(a) A novel configuration of a tuned mass damper (TMD) with energy harvester (PSFAF) of piezoelectric stacks (PS) and force amplification frames (FAF) are introduced where the FAFs for PSs are connected to the TMD'springs in series.

(b) First, The block of TMD's spring and PSFAF can be modeled as an equivalent PS where its constitutive equations are established in the total deformation of the block. After that, the governing equations of TMD-PSFAF attached to an undamped primary structure under external excitation could be derived.

(c) Numerical investigation of the electromechanical system is carried out. It is found that all magnification factors and voltage amplitude curves K_1, K_2, v_0 have fixed points independent of damping, mamely, the curve K_1 has two fixed points *P* and *Q*, the curve K_2 has a fixed point S_2, while the curve v_0 also has a fixed point S_3. K_2 also has a fixed point independent of the resistance ratio α, say S_4. It turns out that S_4 coincides with S_2. Besides, adopting the optimal tuning and damping ratios derived from the fixed point theory applied to the corresponding mechanical TMD, the effective value of α is proposed to be chosen in the interval [1, 2] to achieve vibration suppression for the primary structure as well as harvested voltage amplitude large enough.

(d) Because of the existence of the above-mentioned fixed points, developing the fixed point theory for the proposed energy harvesting TMD configuration will be the further work of this research.

REFERENCES

[1] A. Erturk A., D. J. Inman (2011). Piezoelectric Energy Harvesting. Chichester: Wiley.

[2] N. D. Anh, N. N. Linh, N. Van Manh, V. A. Tuan, N. Van Kuu, A. T. Nguyen, I. Elishakoff (2020). Efficiency of mono-stable piezoelectric Duffing energy harvester in the secondary resonances by averaging method. Part 1: Sub-harmonic resonance. International Journal of Non-Linear Mechanics 126: 103537.

[3] N. N. Linh, A. T. Nguyen, N. Van Manh, V. A. Tuan, N.Van Kuu, N. D. Anh, I. Elishakoff (2021). Efficiency of mono-stable piezoelectric Duffing energy harvester in the secondary resonances by averaging method, Part 2: Super-harmonic resonance. International Journal of Non-Linear Mechanics 137:103817.

[4] De Jong P. H., de Boer A., Loendersloot R., et al. (2013). Power harvesting in a helicopter rotor using a piezo stack in the lag damper. Journal of Intelligent Material Systems and Structures 24(11): 1392-1404.

[5] Zhao S. and Erturk A. (2014). Deterministic and band-limited stochastic energy harvesting from uniaxial excitation of a multilayer piezoelectric stack. Sensors and Actuators A: Physical 214: 58-65.

[6] Feenstra J., Granstrom J. and Sodano H. (2008). Energy harvesting through a backpack employing a mechanically amplified piezoelectric stack. Mechanical Systems and Signal Processing 22(3): 721-734.

[7] Xu T., Jiang X. and Su J. (2011). A piezoelectric ceramic multilayer-stacked hybrid actuation/transduction system. Applied Physics Letters 98(24): 243503.

[8] Zhou W. and Zuo L. (2013). A novel piezoelectric multilayer stack energy harvester with force amplification. In: Proceedings of the ASME 2013 International Design Engineering Technical Conferences, Portland, OR, 4-7 August.

[9] Y. Wang, W. Chen, P. Guzman (2016). Piezoelectric stack energy harvesting with a force amplification frame: Modeling and experiment. Journal of Intelligent Material Systems and Structures, 27(17), 2324-2332.

[10] Secord T. W., Mazumdar A. and Asada H. (2010). A multi-cell piezoelectric device for tunable resonance actuation and energy harvesting. In: Proceedings of the IEEE International Conference on robotics and automation, Anchorage, AK, 3-7 May, pp. 2169-2176. New York: IEEE.

[11] Liu J., O'Connor W., Ahearne E. et al. (2014). Electromechanical modeling for piezoelectric flextensional actuators. Smart Materials and Structures 23: 025005 (13 pp).

[12] Y. Kuang, Z. J. Chew, J. Dunville, J. Sibson, M. Zhu (2021). Strongly coupled piezoelectric energy harvesters: Optimised design with over 100 mW power, high durability and robustness for self-powered condition monitoring. Energy Conversion and Management, 237, 114129.

[13] W. Hendrowati, H.L. Guntur, I.N. Sutantra, Design, modeling and analysis of implementing a multilayer piezoelectric vibration energy harvesting mechanism in the vehicle suspension, Engineering 4 (11), (2012) 728-738.

[14] S. F. Ali, S. Adhikari (2013). Energy Harvesting Dynamic Vibration Absorbers, J. Appl. Mech. 80 (4) 041004.

[15] P. Pan, D. Zhang, X. Nie, H. Chen (2016). Development of piezoelectric energy-harvesting tuned mass damper, Science China Technological Sciences, 60(3), 467-478.

[16] Y. A. Lai, J. Y. Kim, C. S. W. Yang, L. L. L. Chung (2020). A low-cost and efficient d33-mode piezoelectric tuned mass damper with simultaneously optimized electrical and mechanical tuning, J. of Int. Mat. Sys. and Str. 32 (6) 678-696.

[17] Cao D. X., Duan X. J., Guo X.Y., & Lai S. K. (2020). Design and performance enhancement of a force-amplified piezoelectric stack energy harvester under pressure fluctuations in hydraulic pipeline systems. Sensors and Actuators A: Physical, 112031.

[18] N. N. Linh, V. A. Tuan, N. V. Manh, N. D. Anh (2022). Response analysis of undamped primary system subjected to base excitation with a dynamic vibration absorber integrated with a piezoelectric stack energy harvester, Vietnam J. Mech. 44 (4) 490-499.

[19] N. N. Linh, N. D. Anh, L. D. Viet, N. A. Ngoc, V. A. Tuan, T. D. Nang, N. V. Manh (2022). Patent Title: Tuned mass damper with integrated vibrating piezoelectric energy harvester, Intellectual Property Office of Vietnam, Application Number: 1-2022-02620, Publication Number: 1/088043 A, Publication date: 26/07/2022 (in Vietnamese)

[20] Standards Committee of the IEEE Ultrasonics (1987). Ferroelectrics, and Frequency Control Society, IEEE Standard on Piezoelectricity, IEEE, New York.

[21] N. N. Linh (2022). Series combination models of piezoelectric energy harvesters with spring and damper. In the 11th National Conference on Mechanics, Vol. 2. (in Vietnamese).

[22] J. P. Den Hartog (1985). Mechanical Vibrations, Dover, New York, ISBN: 0-486-64785-4.

[23] J. Connor, S. Laflamme (2014). Structural Motion Engineering, Springer International Publishing, Switzerland, ISBN: 978-3-319-06281-5.